# Sensitivity of Silver Square and Triangular Chiral Plasmon Nanosensors

**Akram Kabiri* and Abbas Azarian**

**Department of Physics, University of Qom, Qom, Iran**

***Corresponding author email:** A.kabiri@stu.qom.ac.ir

**Regular paper:** Received: Mar. 10, 2021, Revised: May. 21, 2021, Accepted: Aug. 27, 2021, Available Online: Aug. 29, 2021, DOI: 10.52547/ijop.15.1.65

**ABSTRACT— Plasmonic nanosensors have emerged as a powerful tool for biosensing and other applications. Therefore, efforts are underway to achieve higher sensitivity for these nanosensors. In line with this goal, we have investigated the sensitivity of silver square and triangular chiral nanosensors based on two strategies, Localized Surface Plasmon Resonance (LSPR)-based and Circular Dichroism (CD)-based sensing. Chiral nanostructure parameters (height, diameter) and the angle of incidence light have been optimized with calculation method (3-D finite-difference time-domain (3-D- FDTD)) in order to obtain best localized surface plasmon resonance and consequently the highest sensitivity. The calculation results show that sensitivitys~1727 and 1658nmRIU$^{-1}$ can be achieved in LSPR- and CD-based sensing method respectively for square chiral nanostructure, which are significantly more than previous works.**

**KEYWORDS:** Chiral nanostructure, Plasmonic sensors, High sensitivity, LSPR-based sensing, CD-based sensing, FDTD.

## I. INTRODUCTION

Plasmonic metal nanoparticles have great potential for chemical and biological sensor applications [1]-[4], due to their sensitive spectral response to the local environment of the nanoparticle surface and ease of monitoring the light signal due to their strong scattering or absorption. When a metallic nanostructure is illuminated by incident light of a larger wavelength than the size of the nanostructure, localized electrons in the metallic nanostructure oscillate and create strong surface waves [5]. The curved surface of the particle generates an effective restoring force on the conduction electrons so that resonance can arise. This phenomenon leads to strong field enhancement in the near field zone. This resonance is called LSPR [6], [7]. One of the most remarkable effects of LSPR is that the intensity of LSPR is sensitive to changes of the refractive indices around noble metal nanoparticles [8], [9]. The advantages of LSPR sensors having this characteristic are real-time analysis, label-free detection, and high sensitivities [10]-[12]. The intensity and peak location of the absorption and scattering spectra are highly dependent on the nanoparticle shape, size, and composition as well as the refractive index of the surrounding medium. By taking into account the relationship between the LSPR signal and its influencing factors, there has been significant interest in developing high-sensitivity chemical and biological sensors based on nanostructured platforms [13]-[16].

Theoretical consideration on the surface plasmon resonance condition revealed that the LSPR- based sensing, defined as the relative shift in resonance wavelength with respect to the refractive index change of surrounding materials, has two controlling factors: first the bulk plasma wavelength, a property dependent on the metal type, and second on the aspect ratio of the nanostructures which is a geometrical parameter. It is found that the sensitivity is linearly proportional to both of these factors [17]. In sensor applications high sensitivity of the spectral response of the plasmonic resonance absorption (or scattering) band to the

[ Downloaded from ijop.ir on 2026-11-23 ]

changes in the refractive index of the surroundings is desired. Many theoretical and experimental studies [18]-[21] have been made on metal nanoparticles with different geometry to find the best nanoparticle configuration to enhance the sensitivity of the plasmon resonance response. From the viewpoint of sensitivity, metal nanorod and nanoshell structures have been at the center of attention. Recently, theoretical simulations and experimental data have demonstrated that anisotropic nanostructures exhibit higher refractive index sensitivity [22], [23].

Nowadays, the technique of nanostructures and microstructures allows the construction of precise and skillful shapes, such as three dimensional helix antennas [24]-[27]. Optical response of nanostructures can be adjusted by controlling their size, number of steps or torsion around the central axis, and other geometric parameters.

On the other hand chirality is an intriguing property of certain molecules or artificial nanostructures, which can provide a chiral plasmonic sensing approach. Chiral media have different optical responses to left- and right handed circularly polarized light, and give rise to important optical phenomena such as circular dichroism (CD). CD-based sensing measures the differential extinction between left-handed (LH) and right-handed (RH) circularly polarized light using CD spectroscopy (i.e. $CD \propto E_L - E_R$). The change in response to the change in the refractive index of the medium surrounding the nanoparticles is tracked [28]. CD-based sensing with chiral nanoparticles offers distinct advantages to LSPR- based sensing. CD spectra are naturally consisting of more spectral features compared to an extinction peak that can be tracked when the local environment changes. In particular, the crossing points (CD=0) where the LH and RH extinctions are equal and the signal changes sign are ideal features to track, because they are intrinsically narrow and lead to high figures of merit [29]-[31]. In addition, chiral plasmonic structures have a higher degree of flexibility in terms of spectral tenability.

## II. Structure and Analysis Method

The helix structures under study are schematically presented in Fig. 1. They consist of a constant side length ($L$=140 nm). The structural period and angle of the rise of the structures are $h=3L\mathrm{Sin}(\theta)$ and $\theta=\pi/4$, respectively. We consider $a$ uniform environment with refractive index $n$=1 around each nanostructure. The square and triangular helix structures are illuminated by circular polarized wave in the wavelength ranges $200<\lambda<2400$ and $200<\lambda<2000nm$, respectively at incidence angle of φ=0 to the z-axis with polarization in the direction of the x-axis. The calculations are performed with 3D finite difference time domain (FDTD) [32].

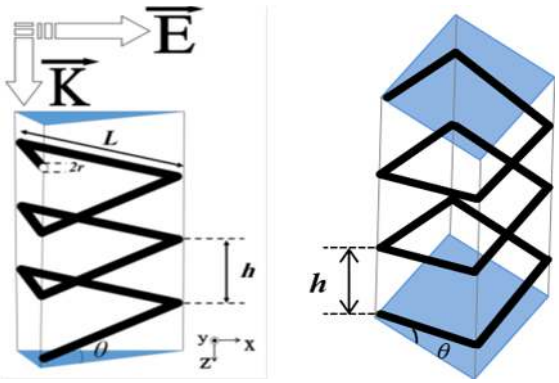


Fig. 1. Schematic model and geometric parameters of the square and triangular chiral plasmon nanosensors.

## III. Optimization

In this section, at first we try to find the best angle of incidence light that leads to a narrow and long resonance peak. Then we investigate the effects of geometric parameters of triangular helix-structure (number of steps (height) and radius) on refractive index sensitivity which is defined as the ratio of resonant wavelength shift $\Delta\lambda(nm)$ to the variation of surrounding refractive index $\Delta n$

$$S=\frac{\Delta\lambda(nm)}{\Delta n(RIU)} \quad (1)$$

### A. *The Dependence of Light Beam Angle*

We start by optimizing the angle of incident light ($\varphi$) in order to find the best LSPR

[ Downloaded from ijop.ir on 2026-11-23 ]

responses. This can be essential, as a quality peak can increase the resolution of spectrum. For this purpose, we consider scattering cross-section of silver triangular helix-structure (THS) at different incident light angle and choose the structure radius $r$=5$nm$ and number of steps=3. Figure 2 shows a comparison of the scattering spectra for the incident angles $\varphi = 0°, 45°$ and $90°$ . Incident angle substantially modifies the LSPR peak position and intensity and it is observed that for incident angle of $\varphi = 0^{\circ}$ the resonance is significantly stronger than other angles.

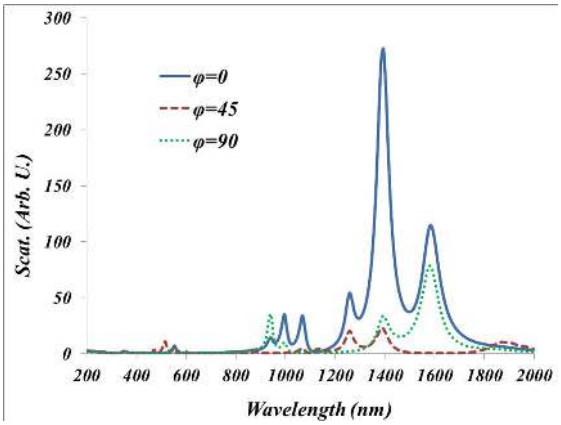


Fig. 2. Simulated scattering spectra of triangular helix-structure for various incidence angles ( $\varphi = 0^{\circ}, 45^{\circ}$ and $90^{\circ}$ )

## B. *The Dependence of Number of Steps*

Second, we compare the refractive index sensitivity of THSs for different number of steps from 1 to 3. Figure 3 shows the scattering spectra at normal incidence light ( $\varphi = 0^{\circ}$ ) for THS with $r$=5$nm$, number of steps=1 and refractive index=1, 1.1, 1.2, and 1.33 as sample. As can be seen the scattering cross-sections have a single peak, which means the existence of dipolar particle plasmons. These peaks are specific to the dipolar distribution of conducting electrons relative to positive charge of the field. There is also a red shift in the spectrum with increasing the refractive index and a sensitivity of S=1095 nm/RIU is obtained according to Eq. (1).

Similarly, the sensitivity for THSs with 2 and 3 steps are calculated and compared in the Fig. 4, which are equal to 1287 and 1346 nm/RIU respectively. It is found that if the radius is constant, the sensitivity increases with increasing number of steps (height).

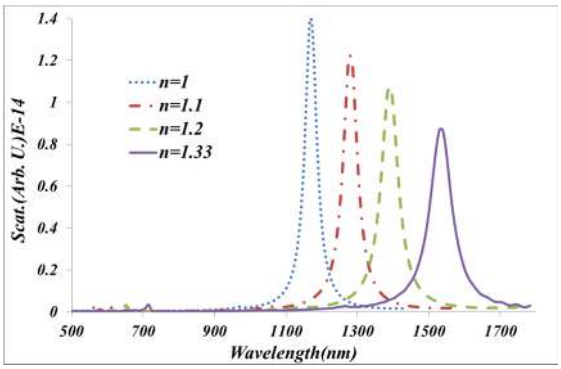


Fig. 3. Scattering cross-sections of THS under normal incidence light for various refractive index from 1 to 1.33. number of steps=1 and structure radius=5nm are fixed.

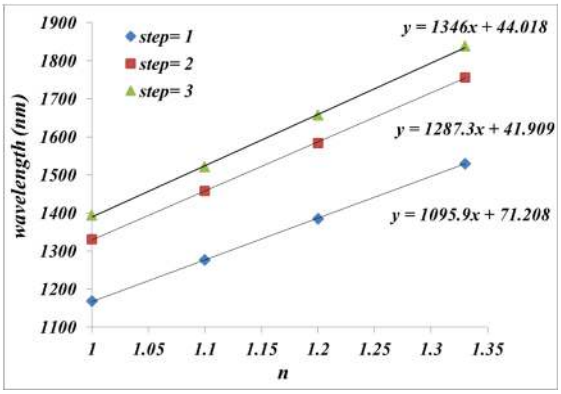


Fig. 4. The wavelength of LSPR peaks Vs. the refractive index of the surrounding medium for THS with different number of steps from 1 to 3. Structure radius=5nm is fixed.

## C. *The Dependence of Radius*

Third, we study the dependence of sensitivity on the THS radius. Scattering cross-section at normal incident light for THS with $r$=5nm and number of steps=3 is presented in Fig. 5. The resonant wavelength shifts significantly with respect to refractive index change and obtain a sensitivity equivalent to $S$ =1346 nm/RIU.

On the other hand, a comparison of Figs. 3 and 5 shows that for each given refractive index, there is a read shift (resonance peak occur at longer wavelength) with increasing aspect ratio (length to radius ratio) of nanostructure which is due to reduce amount of the net dipole-moment.

[ Downloaded from ijop.ir on 2026-11-23 ]

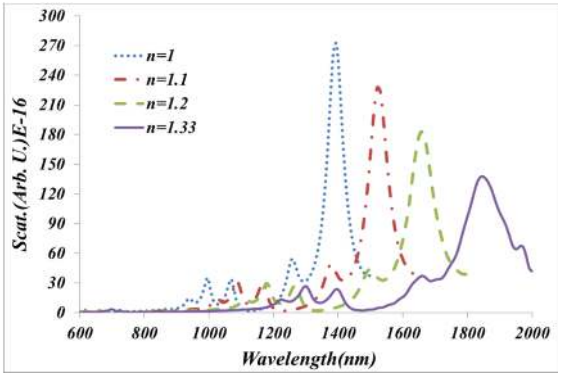


Fig. 5. Scattering cross-sections of THS under normal incidence light for various refractive index from 1 to 1.33. Number of steps=3 and structure radius = 5nm are fixed.

Figure 6 presents the wavelength of LSPR peaks versus the refractive index of the surrounding medium for THSs with number of step=3 and different radius *(r*=5*,* 10*,* 15, and 20 *nm)*. Our results show, if the number of steps is constant, the sensitivity decreases with increasing nanoparticle radius. The highest sensitivity is obtained for THS with number of step=3 and *r*=5nm and is equal to 1346 nm/RIU.

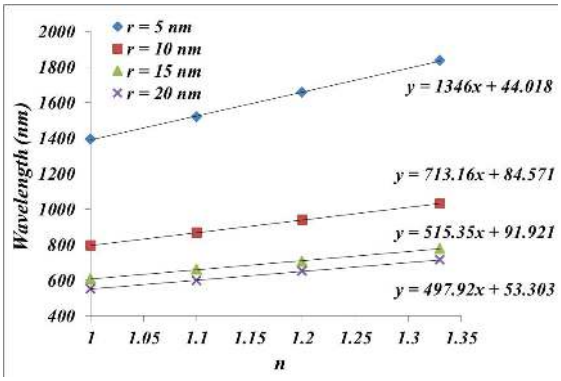


Fig. 6. The wavelength of LSPR peaks Vs. the refractive index of the surrounding medium for THS with different radius from *r*=1nm to 20nm. Number of steps=3 is fixed.

## IV. Sensitivity of Square-Helix Structure

In the previous section, we optimized the geometric parameters of the nanostructure to achieve greater sensitivity. The plasmon sensitivity in wavelength units shows the expected steady increase for an increasing aspect ratio. So, in this section based on the optimal parameters (The largest aspect ratio for square helical structure that our computational facilities let us to simulate.) we calculate the sensitivity for square helix-structure (SHS) using two strategies, LSPR- and CD-based sensing.

### *A. LSPR-based Sensing*

Scattering cross-sections for SHS with number of step=3, r=5nm and different refractive index (n=1, 1.1, 1.2, and 1.33) are plotted in Fig. 7. Main plasmon band consist of three peaks, which can indicate multipolar of higher orders (quadrupole, octopole and …). We consider the middle peak (the highest peak) to calculate the sensitivity and a value as large as S=1727nm/RIU is obtained for it which is significantly higher than the sensitivity of TSH.

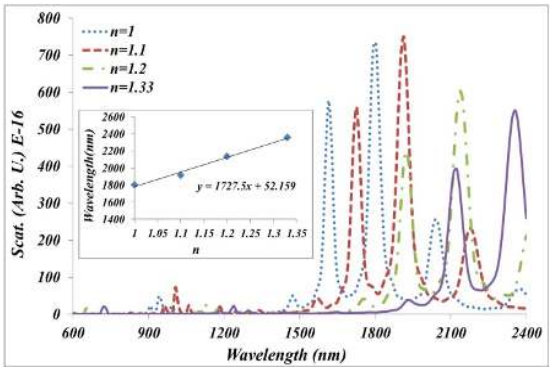


Fig. 7. Scattering cross-sections of SHS with number of steps=3 and structure radius *r*=5nm under normal incidence light for various refractive index from 1 to 1.33. Inset: The wavelength of LSPR peaks Vs. the refractive index of the surrounding medium.

### A. *CD-based Sensing*

We also examined other strategy for calculating the sensitivity of SHS. First, we calculate the scattering spectra of SHS for right- and left-handed circularly polarized light under normal incidence. Then the CD spectra of the structure can be calculated as $CD = (scat)_L - (scat)_R$ that is shown in Fig. 8. As expected, the CD spectra show multiple features. We track the CD spectra at the maximum $(\lambda_M)$, zero crossing $(\lambda_0)$ and minimum $(\lambda_m)$ in response to changes in the refractive index of the surroundings.

The wavelength shifts relative to refractive index are presented in Fig. 9. For $\lambda_M$, $\lambda_o$ and

[ Downloaded from ijop.ir on 2026-11-23 ]

$\lambda_m$ the sensitivity is equal to 1600, 1603 and 1658nm/RIU respectively. All three are almost of the same order and large enough for sensor applications.

It is noteworthy that in our previous work [33] we calculated the sensitivities for the three CD spectral features of triangular helical structure as 1718, 1492 and 1372 nm/RIU For $\lambda_M$, $\lambda_o$ and $\lambda_m$ respectively.

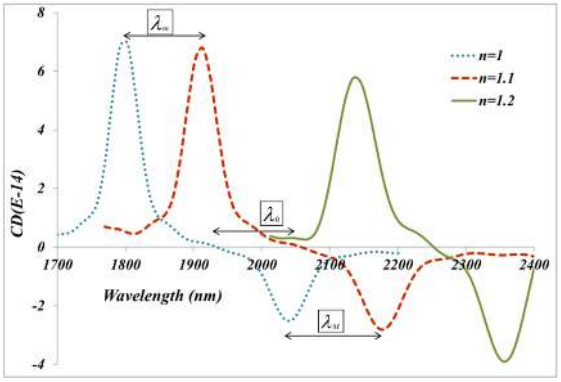


Fig. 8. CD spectra of the SHS with number of steps = 3 and structure radius $r$=5nm Vs. wavelength for the different refractive index of the surrounding medium.

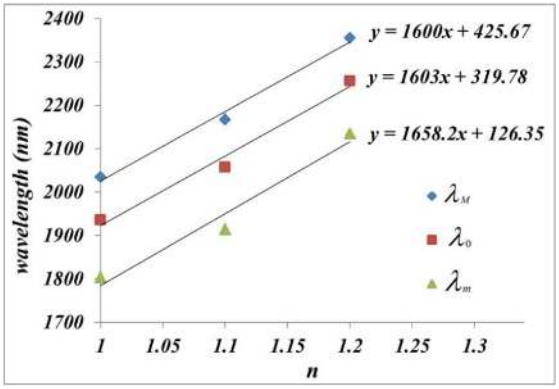


Fig. 9. The wavelength shifts relative to refractive index of the surrounding medium for $\lambda_M$, $\lambda_o$ and $\lambda_m$

## V. Conclusion

In this work, we simulated the spectral characteristics of plasmonic resonance in square and triangular helix-structure based on 3-D-FDTD method. We first optimized the light beam incidence angle and geometric parameters (number of steps and radius) of triangular helix-structure in order to achieve the highest sensitivity. The simulation results show that, the best angle of incidence light is $\varphi = 0^\circ$ and also we concluded that, the sensitivity increases with increasing aspect ratio. Furthermore, we calculated the sensitivity for square helix-structure with three steps and $r$=5nm. Our results showed that both LSPR-based sensing and CD-based sensing have ultra-high sensitivity (1727 and 1658nm/RIU respectively), which are significantly larger than other's works [34] and make this structure ideal for sensor applications.

## References

**[1]** D.A. Stuart, A.J. Haes, C.R. Yonzon, E.M. Hicks, and R.P. Van Duyne "Biological applications of localized surface plasmonic phenomenae," IEE Proc Nanobiotechnol, Vol. 152, pp. 13-32, 2005.

**[2]** I.H. El-Sayed, X. Huang and M.A. El-Sayed "Surface plasmon resonance scattering, and absorption of anti-EGRF antibody conjugated gold nanoparticles in cancer diagnostics," Nano Lett, Vol. 5, pp. 829-834, 2005.

**[3]** L. Cognet, C. Tardin, D. Boyer, D. Choquet, and P. Tamarat, "Single metallic nanoparticle imaging for protein detection in cells," B. Proc. Natl. Acad. Sci. U.S.A, Vol. 100, pp. 11350-11355, 2003.

**[4]** A.D. McFarland and R.P. Van Duyne, "Single silver nanoparticles as real-time optical sensors with zeptomole sensitivity," Nano Lett. Vol. 3, pp. 1057-1062, 2003.

**[5]** B. Liedberg, C. Nylander, and I. Lunstrom, "Surface plasmon resonance for gas detection and biosensing," Sens. Actuat. Vol. 4, pp. 299-304, 1983.

**[6]** J. Langer, S.M. Novikov, and L.M. Liz-Marzan "Sensing using plasmonic nanostructures and nanoparticles," Nanotechnology, Vol. 26, pp. 322001 (1-28), 2015.

**[7]** M. Manzano, P. Vizzini, K. Jia, P.M. Adam, and R.E. Ionescu, "Development of localized surface plasmon resonance biosensors for the detection of Brettanomyces bruxellensis in wine," Sens. Actuators B Chem, Vol. 223, pp. 295–300, 2016.

**[8]** A.B. Dahlin, J.O. Tegenfeldt, and F. Hook "Improving the instrumental resolution of sensors based on localized surface plasmon

[ Downloaded from ijop.ir on 2026-11-23 ]

resonance," Anal. Chem. Vol. 78, pp. 4416–4426, 2006

**[9]** H.M. Kim, K.T. Nam, S.K. Lee, and J.H. Park, "Fabrication and measurement of microtip array-based LSPR sensor using bundle fber," Sens. Actuat. A Phys. Vol. 271, pp. 146–152, 2018.

**[10]** S.K. Srivastava, R.K. Verma, and B.D. Gupta, "Theoretical modeling of a localized surface plasmon resonance based intensity modulated fiber optic refractive index sensor," Appl. Opt. Vol. 48, pp. 3796–3802, 2009.

**[11]** H.H. Jeong, N. Erdene, J.H. Park, D.H. Jeong, H.Y. Lee, and S.K. Lee, "Real-time label-free immunoassay of interferon-gamma and prostate-specific antigen using a fiber-optic localized surface plasmon resonance sensor," Biosens. Bioelectron. Vol. 39, pp. 346–351, 2013.

**[12]** L. Xie, X. Yan, and Y. Du, "An aptamer based wall-less LSPR array chip for label-free and high throughput detection of biomolecules," Biosens. Bioelectron. Vol. 53, pp. 58–64, 2014.

**[13]** K.M. Mayer and J.H. Hafner, "Localized Surface Plasmon Resonance Sensors," Chem. Rev. Vol. 111, pp. 3828-3857,2011.

**[14]** B. Sepúlveda, P.C. Angelomé, L.M. Lechuga, and L.M. Liz-Marzán, "LSPR-based nanobiosensors," Nano Today, Vol. 4, pp. 244-251, 2009.

**[15]** Y. Chen and H. Ming, "Review of surface plasmon resonance and localized surface plasmon resonance," Photonic Sensors, Vol. 2, pp. 37-49, 2012.

**[16]** H. Jans and Q. Huo, "Gold nanoparticle-enabled biological and chemical detection and analysis," Chem. Soc. Rev. Vol. 41, pp. 2849-2866, 2012.

**[17]** K.S. Lee and M.A. El-Sayed, "Gold and Silver Nanoparticles in Sensing and Imaging: Sensitivity of Plasmon Response to Size, Shape, and Metal Composition," J. Phys. Chem. B, Vol. 110, pp. 19220-19225, 2006.

**[18]** K.L. Kelly, E. Coronado, L. Zhao, and G.C. Schatz, "The Optical Properties of Metal Nanoparticles: The Influence of Size, Shape, and Dielectric Environment," J. Phys. Chem. B, Vol. 107, pp. 668-677, 2003.

**[19]** F. Tam and C. Moran, "Geometrical Parameters Controlling Sensitivity of Nanoshell Plasmon Resonances to Changes in Dielectric Environment," J. Phys. Chem. B, Vol. 108, pp. 17290-17294, 2004.

**[20]** G. Raschke, S. Brogl, A.S. Susha, A.L. Rogach, T.A. Klar, J. Feldmann, and B. Fieres, "Gold Nanoshells Improve Single Nanoparticle Molecular Sensors," Nano Lett. Vol. 4, pp. 1853-1857, 2004.

**[21]** A. Gole and C. J. Murphy, "Seed-Mediated Synthesis of Gold Nanorods: Role of the Size and Nature of the Seed," Chem. Mater, Vol. 16, pp. 3633-3640, 2004.

**[22]** K.S. Lee and M.A. El-Sayed, "Gold and Silver Nanoparticles in Sensing and Imaging: Sensitivity of Plasmon Response to Size, Shape, and Metal Composition," J. Phys. Chem. B, Vol. 110, pp. 19220-19225, 2006.

**[23]** P.K. Jain, K.S. Lee, I.H. El-Sayed, and M.A. El-Sayed, "Calculated Absorption and Scattering Properties of Gold Nanoparticles of Different Size, Shape, and Composition: Applications in Biological Imaging and Biomedicine," J. Phys. Chem. B, Vol. 110, pp. 7238-7248, 2006.

**[24]** C. Helgert, E. Pshenay-Severin, M. Falkner, Ch. Menzel, C. Rockstuhl, E.-B. Kley, A. Tünnermann, F. Lederer, and T. Pertsch, "Chiral metamaterial Composed of Three Dimensional Plasmonic Nanostructures," Nano Lett. Vol. 11, pp. 4400-4404, 2011.

**[25]** B. Frank, "Large Area 3D Chiral Plasmonic Structures," ACS Nano, Vol. 7, pp. 6321-6329, 2013.

**[26]** A. Belardini, A. Benedetti, M. Centini, G. Leahu, F. Mura, S. Sennato, C. Sibilia, V. Robbiano, M. Caterina Giordano, Ch. Martella, D. Comoretto, and F. Buatier de Mongeot, "Second Harmonic Generation Circular Dichroism from Self Ordered Hybrid Plasmonic-Photonic Nanosurfaces," Adv. Opt. Mater, Vol. 2, pp. 208-213, 2014.

**[27]** M. Esposito, V. Tasco, M. Cuscunà, F. Todisco, A. Benedetti, I. Tarantini, M. De Giorgi, D. Sanvitto, and A. Passaseo, "Nanoscale 3D Chiral Plasmonic Helices with Circular Dichroism at Visible Frequencies," ACS Photon, Vol. 2, pp. 105-114, 2015.

**[28]** H.H. Jeong, A.G. Mark, and P. Fischer, "Magnesium plasmonics for UV applications and chiral sensing," Chem. Commun. Vol. 52, pp. 12179-12182, 2016.

[ Downloaded from ijop.ir on 2026-11-23 ]

**[29]** E. Hendry, T. Carpy, J. Johnston, M. Popland, R. Mikhaylovskiy, A. Lapthorn, S. Kelly, L. Barron, N. Gadegaard, and M. Kadodwala, "Ultrasensitive detection and characterization of biomolecules using superchiral fields," Nat. Nanotechnol, Vol. 5, pp. 783–787, 2010.

**[30]** V.K. Valev, J.J. Baumberg, C. Sibilia, and T.Verbiest, "Chirality and chiroptical effects in plasmonic nanostructures: fundamentals, recent progress, and outlook," Adv. Mater. Vol. 25, pp. 2517–2534, 2013.

**[31]** S. Zhang, J. Zhou, Y.-Sh. Park, J. Rho, R. Singh, S. Nam, A Azad, H.-T. Chen, X. Yin, A. J. Taylor, and X. Zhang, "Photoinduced handedness switching in terahertz chiral metamolecules," Nat. Commun. Vol. 3, pp. 942-958, 2012.

**[32]** S.A. Palkar, N.P. Ryde, M.R. Schure, and N. Gupta, "Finite Difference Time Domain Computation of Light Scattering by Multiple Colloidal Particles," Langmuir, Vol. 14, pp. 3484-3492, 1998.

**[33]** A. Azarian and A. Kabiri, "Ultrahigh sensitive silver trigonal chiral nanosensors," Optik, Vol. 224, pp. 165663, 2020.

**[34]** H.H. Jeong, A.G. Mark, M.A. Correa, I. Kim, P. Oswald, T.C. Lee, and P. Fischer, "Dispersion and shape engineered plasmonic nanosensors," Nature Commun. Vol. 7, pp. 11331 (1-7), 2016.



**Abbas Azarian** graduated in condensed mater physics at the Sharif University of Technology (SUT), Iran, in 2005. He received his Ph.D. in Nano-optics from the SUT in 2009. He is currently Associate Professor at the Physics Department, University of Qom, Iran. His research activity mainly focuses on the Nano optical sensors.



**Akram Kabiri** received her Master degree in condensed mater physics from Esfahan University in 2011 and now she is keeping on her researches as a Ph.D. student in Qom University. Her current research interests include: Plasmonic and Nanosensors.

[ Downloaded from ijop.ir on 2026-11-23 ]

**THIS PAGE IS INTENTIONALLY LEFT BLANK.**

[ Downloaded from ijop.ir on 2026-11-23 ]